esa ECOSPHERE

Leaf ^{13}C data constrain the uncertainty of the carbon dynamics of temperate forest ecosystems

SHAOQING LIU[1,2] AND QIANLAI ZHUANG[1,3,]†

[1]*Department of Earth, Atmospheric and Planetary Sciences, Purdue University, West Lafayette, Indiana, USA*
[2]*Department of Environmental and Earth Sciences, University of Minnesota, Twin Cities, Minneapolis, Minnesota, USA*
[3]*Department of Agronomy, Purdue University, West Lafayette, Indiana, USA*

Citation: Liu, S., and Q. Zhuang. 2021. Leaf ^{13}C data constrain the uncertainty of the carbon dynamics of temperate forest ecosystems. Ecosphere 12(10):e03741. 10.1002/ecs2.3741

Abstract. Stable carbon isotope discrimination occurred in plant biophysical and biogeochemical processes can help understand plant physiology and soil biogeochemistry with respect to carbon cycling. Here, we incorporated the photosynthetic carbon isotope discrimination into a process-based land surface model (iTEM) to test if stable carbon isotope composition ($\delta^{13}C$) can impose additional constraint on model parameters. Sequential data assimilation was implemented at six eddy covariance flux tower sites using carbon flux observations including gross primary productivity (GPP) and net ecosystem exchange (NEE) with and without considering foliar $\delta^{13}C$ ($\delta^{13}C_f$) measurement constraints, respectively. Our model-data fusion showed that $\delta^{13}C_f$ can provide useful constraint on photosynthetic (V_{cmax25}, the maximum rate of carboxylation at 25°C) and stomatal ($g1$, the slope of stomatal function) parameters as well as the posterior carbon fluxes. When including $\delta^{13}C_f$ measurement, $g1$ spatially varies among the six sites and is significantly correlated with annual precipitation. We incorporated the statistical relationship between $g1$ and annual precipitation into iTEM, which is then used to quantify the regional carbon dynamic in temperate forest ecosystems of the Northern Hemisphere. Compared with the simulation only conditioned on carbon flux observations, regional carbon flux estimations performed slightly better against the FLUXCOM products and the uncertainties of modeled carbon fluxes were reduced by 27%. Our study demonstrated that $\delta^{13}C_f$ data constrains carbon flux uncertainties across space.

Key words: carbon fluxes; data assimilation; land surface models; model uncertainty; stable carbon isotope.

Received 27 March 2021; accepted 6 April 2021. Corresponding Editor: Debra P. C. Peters.

† **E-mail** : qzhuang@purdue.edu

INTRODUCTION

Quantification of ecosystem carbon fluxes and their responses to environmental changes would improve our understanding of carbon-climate feedbacks. Land surface models (LSM) incorporated with key biophysical and biochemical processes, including photosynthesis, respiration, and evapotranspiration, are important tools to predicting carbon exchanges between terrestrial biosphere and the atmosphere (IPCC 2014). To date, the model-data fusion approach encompassing model parameter optimization and uncertainty quantification using eddy flux tower observation (e.g., carbon and water fluxes) has been widely used for quantifying ecosystem responses to changing climate (Williams et al. 2009).

As an important tracer in the biogeochemical process, the stable carbon isotope composition (designated as $\delta^{13}C$) provides novel insights on plant physiological, soil biological, physical, and chemical processes (Brüggemann et al. 2011) and is potentially useful to constrain the process-based ecosystem models. The carbon isotope composition in atmospheric CO_2 (designed as

$\delta^{13}C_{atm}$) has been used to provide an additional constraint on carbon budget quantifications (Tans et al. 1993, Ciais et al. 1995) and to examine the relative contribution of C3 and C4 plants to total primary productivity (Sage et al. 1999, Griffis et al. 2010). At the local scale, the $\delta^{13}C$ measurement has been adopted in ecological research as integrators of how organisms interact with and respond to the abiotic and biotic environment changes. For example, the $\delta^{13}C$ variation of plant tissue can improve our understanding on the response of plants to changes in precipitation, vapor pressure deficit (Farquhar and Richards 1984, Bowling et al. 2002, Diefendorf et al. 2010) and the intrinsic water use efficiency (Saurer et al. 2004, Seibt et al. 2008). In addition, the high-frequency in situ carbon isotopic flux measurement provides a novel tool to partitioning the net ecosystem exchange (NEE) into photosynthesis and respiration (Bowling et al. 2001).

Abundant in situ foliar $\delta^{13}C$ (designated as $\delta^{13}C_f$) measurements have been published and the relationship between the $\delta^{13}C_f$ variation and environmental conditions (Marshall et al. 2007), edaphic factors (Arens et al. 2000) and plant attributes (Kaplan et al. 2002) has been well documented. A theoretical treatment of carbon isotope discrimination (the offset between $\delta^{13}C_{atm}$ and $\delta^{13}C_f$, designated as Δ) in C3 and C4 vegetation photosynthesis (Farquhar and Richards 1984) has been incorporated into modeling to estimate plant carbon discrimination at different spatial and temporal scales (Fung et al. 1997, Suits et al. 2005, Scholze et al. 2008). As for the ^{13}C fractionation process during photosynthesis, the photosynthetic fractionation in C3 plant is modeled as:

$$\Delta = a\frac{C_a - C_s}{C_a} + b\frac{C_s - C_i}{C_a} + c\frac{C_i - C_c}{C_a} + d\frac{C_c}{C_a}$$

where a (2.9‰), b (4.4‰), c (1.8‰), and d (28.2‰) are constants representing fractionation due to diffusion at the boundary layer, stomatal cavity, CO_2 entering solution and Rubisco CO_2 fixation, respectively. C_a, C_s, C_i, and C_c are the CO_2 concentration in the air, at the boundary layer, stomata, and chloroplast, respectively. In literature, a simplified two-stage (diffusion and carboxylation) model is often applied to estimate photosynthetic carbon isotope fractionation:

$$\Delta = A + (B - A) \times \frac{C_i}{C_a}$$

where A (4.4‰) and B (28‰) are constants representing fractionation due to diffusion and carboxylation, respectively. According to Farquhar photosynthesis formula (Farquhar et al. 1980), the carbon assimilation rate is a function of the intercellular CO_2 concentration (C_c or C_i), and therefore, the in situ observation of carbon fluxes combined with the measurements of isotopic signal of plant tissues, which integrate all the biophysical and biogeochemical processes, may have good constraints on the parameters related to biophysical and biochemical processes at the canopy scale. Previous studies have attempted to combine in situ $\delta^{13}C_f$ measurement for calibrating LSMs (Aranibar et al. 2006; Raczka et al. 2016; Duarte et al. 2017). For example, Aranibar et al. (2006) found that the annual integrated $\delta^{13}C_f$ could place additional constraints on relevant parameters of stomatal conductance model at a needleleaf forest site. However, these studies mainly focused on single site and only one plant functional type (PFT) (temperate evergreen forest). It is not clear whether $\delta^{13}C_f$ can help optimize parameters in LSM at other sites with different climates and vegetation types.

This study is to assess if $\delta^{13}C_f$ measurement can constrain the key parameters related to the carbon fluxes at multiple forest sites for a process-based LSM (iTEM; Chen and Zhuang 2014, Liu et al. 2014, 2016). By implementing a rigorous model-data fusion approach using observation of both carbon flux and $\delta^{13}C_f$ observations, we aimed at addressing two questions: (1) Can $\delta^{13}C_f$ measurement consistently improve model parameterization across multiple sites? (2) What are the regional implications to carbon fluxes when $\delta^{13}C_f$ is included as an additional constraint to model parameters?

Data and Methods

Land surface model (iTEM) and photosynthetic fractionation process

In the integrated Terrestrial ecosystem model (iTEM), the canopy is modeled with a one-layer, two-big-leaf approach (Dai et al. 2004), which diagnoses energy budget, leaf temperature, evapotranspiration, and photosynthesis separately for

sunlit and shaded leaves. The boundary layer turbulent processes are modeled based on the Monin-Obukhov similarity theory. The hydrological processes include the interception, through fall of precipitation, snow accumulation, sublimation and melt, surface runoff, surface evapotranspiration, water infiltration, and redistribution in soil and subsurface drainage. These algorithms allow the model to simulate the response of land surface processes to changing direct and diffusive radiation regimes, such as surface energy balance, thermal dynamics, leaf and canopy conductance, and surface evapotranspiration. In addition, the iTEM kept the approach of TEM in modeling ecosystem carbon and nitrogen dynamics and their interactions (Zhuang et al. 2003). Two carbon pools and four nitrogen pools are used to represent carbon and nitrogen pools in a terrestrial ecosystem, including vegetation carbon, soil organic carbon, vegetation labile nitrogen, vegetation structural nitrogen, soil organic nitrogen, and soil inorganic nitrogen. More details of the iTEM are documented in Chen (2013).

As for the ^{13}C discrimination process during photosynthesis, the ^{13}C fractionation during photosynthesis is modeled as:

$$\Delta = a\frac{C_a - C_s}{C_a} + b\frac{C_s - C_i}{C_a} + c\frac{C_i - C_c}{C_a} + d\frac{C_c}{C_a} \quad (1)$$

$$C_s = C_a - \frac{A}{g_b};\ C_i = C_s - \frac{A}{g_s};\ C_c = C_i - \frac{A}{g_m} \quad (2)$$

$$\delta^{13}C_A = \left(\frac{\delta^{13}C_{atm} - \Delta}{1000 + \Delta}\right) \times 1000 \quad (3)$$

where a (2.9‰), b (4.4‰), c (1.8‰), and d (28.2‰) were constants representing fractionation due to diffusion at the boundary layer, stomatal cavity, CO_2 entering solution and Rubisco CO_2 fixation, respectively. g_b is the boundary layer conductance, and C_a, C_s, C_i, and C_c represented the CO_2 concentration in the air, at the boundary layer, stomata, and chloroplast, respectively. We followed Evans and von Caemmerer (1996), assuming mesophyll conductance (g_m) is proportional (4800) to the Rubisco content (V_m). $\delta^{13}C_{atm}$ was assumed as constant (−7.8‰) (White et al. 2015). It was not clear how the post-photosynthetic fractionation and leaf carbon allocation would affect $\delta^{13}C_f$, here we assumed that $\delta^{13}C_f$ equals the isotopic composition of assimilated carbon ($\delta^{13}C_A$) (Aranibar et al. 2006). More detailed steps about the incorporation of $\delta^{13}C_f$ into iTEM can be found in the Appendix S1.

Data

We selected six temperate forest sites from the European Flux network (Table 1, http://www.europe-fluxdata.eu/home). The in situ observed vapor pressure, air temperature, incoming radiation, wind speed, and air pressure were used to drive iTEM. The daily time step net ecosystem exchange (NEE) measurement using the eddy covariance method were from the Level 4 dataset. The NEE data were previously friction-velocity-filtered, gap-filled, and partitioned into the component fluxes of gross primary productivity (GPP) and ecosystem respiration (Reco) using an online tool (http://www.bgc-jena.mpg.de/~MDIwork/eddyproc/, Reichstein et al. (2005)). Here we used the gap-filled NEE values (and derived GPP) based on the marginal distribution sampling method for model-data fusion experiment.

The foliar ^{13}C compositions ($\delta^{13}C_f$) at the six sites were obtained from the Work Package 5 (WP5, entitled "Isotopic Studies") of

Table 1. Forest sites used for model-data fusion.

Site name	Location	Vegetation type	Reference
NLLoo	52.17° N, 5.74° E	ENF	Dolman et al. (2002)
CZBK1	49.50° N, 18.53° E	ENF	Reichstein et al. (2005)
DEHai	51.07° N 10.45° E	DBF	Knohl et al. (2003)
DETha	47.38° N, 8.37° E	ENF	Bernhofer (2003)
ITCol	41.84° N, 13.58° E	DBF	Valentini et al. (1996)
ITNon	44.69° N 11.09° E	DBF	Rebmann et al (2005)

Notes: DBF, deciduous broadleaf forest; ENF, evergreen needleaf forest.

CARBOEUROFLUX project (http://www.weizmann.ac.il/EPS/wp5/results.html). One of the WP5 goals is to monitor and elucidate the ecosystem-scale processes by analyzing the carbon isotope signal in organic tissues as indicators for ecophysiological response to environmental change. The foliar samples were generally taken from the dominant species at the sites with 2–3 fully expanded and sunlight leaves at the top canopy (https://www.weizmann.ac.il/EPS/wp5/sample.html). Compared with the continuous measurement of carbon fluxes (NEE) at these sites, the $\delta^{13}C_f$ measurements were conducted every one or two months during growing season. The observed $\delta^{13}C_f$ values of sunlit leaves reflected the integral of photosynthetic discrimination, expressed by the Eq. 3 above.

For the regional simulations, model runs were conducted at a 3-hourly time step for the period 2003–2010 and at a spatial resolution of 1°×1° for the temperate forest region in the Northern Hemisphere. The meteorological data of air temperature, wind speed, radiation, CO_2, precipitation, water vapor concentration and surface air pressure, the initial conditions, soil properties, and the vegetation distribution were from Chen and Zhuang (2014).

Data assimilation and experiment setup

Our model-data fusion framework employed the ensemble Kalman Filter (EnKF) (Evensen 1994) with an augmented state formulation that allows model parameters to be estimated (Evensen 2009). EnKF incorporates an ensemble of forecasts to estimate background error covariance, which is a Monte Carlo approximation to the traditional Kalman filter. Then, an analysis step improves the forecast by calculating an updated ensemble of model vectors based on available observations:

$$X_t^a = X_t^f + K(y_t - HX_t^f) \tag{4}$$

where

$$K = P_t^f H^T (HP_t^f H^T + R)^{-1} \tag{5}$$

$\boldsymbol{K}$ is the Kalman gain. x_t^f and x_t^a are both augmented model state vectors that comprise model states ($\boldsymbol{S}$) and parameters ($\boldsymbol{p}$) for each ensemble ($\boldsymbol{i}$) before and after the analysis step, respectively. $\boldsymbol{y_t}$ is the observation vector, and $\boldsymbol{H}$ is the operator converting the model states to observation space. P_t^f is the background error covariance matrix, and $\boldsymbol{R}$ is the observation error covariance matrix. Five vegetation related parameters in iTEM were selected for estimation at our selected sites (Table 2). These parameters were found to be sensitive in Chen and Zhuang (2014). The prior parameter distributions were assumed to be uniformly distributed with the range of values reported in White et al. (2000). The EnKF implementation then used two types of data ($\boldsymbol{y}$) for the analysis step, gross primary productivity (GPP) and net ecosystem exchange (NEE) (E0 experiment). To assess if $\delta^{13}C_f$ can further constrain iTEM parameters, another EnKF experiment was implemented using both GPP, NEE and available $\delta^{13}C_f$ observation at these sites (E1 experiment). Based on preliminary EnKF results, an ensemble size of 100 was chosen as a balance of performance and computational feasibility. The data assimilation period started from 2001 to 2002 for all six sites and the conditioned parameters at the final time step for the two EnKF implementations were used for posterior site-level simulations and regional extrapolations. Since EnKF had to forecast the model output for 100 times at each time step, we explored the OPENMPI tool to write the above EnKF algorithm as parallel mode to reduce

Table 2. Selected iTEM parameters for model-data fusion.

Parameter	Unit	Definition	Prior range
V_{cmax25}	μmol $CO_2 \cdot m^{-2} \cdot s^{-1}$	Maximum carboxylation rate at 25 C	[10,150]
N_{fall}	g $N \cdot m^{-2} \cdot s^{-1}$	Litter fall rates of N	$[1,100] \times 10^{-8}$
N_{max}	g $N \cdot m^{-2} \cdot s^{-1}$	Rate of N uptake	$[1,100] \times 10^{-7}$
N_{up}	g/g	Amount of N immobilized per unit of detrital C respired	[0,0.5]
$g1$	/	Empirical coefficient for the sensitivity of stomatal conductance to photosynthesis, CO_2 concentration and relative humidity (Ball-Berry model)	[1,18]

the computation cost. More details about EnKF can be found in the Appendix S1.

Results and Discussions

Data-conditioned parameters and posterior site-level simulations

Results in Fig. 1 show the data-conditioned parameters at each site with the two model-data fusion experiments. Both E0 and E1 had similar estimates in the nitrogen related parameters (N_{fall}, N_{max} and N_{up}), but with different V_{max25} and $g1$ values. In addition, the uncertainties of V_{max25} and $g1$ were narrowed to smaller ranges at all sites when $\delta^{13}C_f$ observations were assimilated in iTEM. For example, the V_{max25} of DeTha site was estimated to range from 60 to 77 μmol $CO_2 \cdot m^{-2} \cdot s^{-1}$ when only GPP and NEE were assimilated into iTEM (Fig. 1; E0 experiment), while its uncertainty can be reduced with additional $\delta^{13}C_f$ observation constraint (E1 experiment), ranging from 63 to 71 μmol $CO_2 \cdot m^{-2} \cdot s^{-1}$. However, the uncertainties of nitrogen parameters (N_{fall}, N_{max}, and N_{up}) did not change significantly, this may be because: (1) The three parameters were relatively well constrained in E0; and/or (2) their variability had negligible effects on $\delta^{13}C_f$ simulations.

Figs. 2, 3, respectively, show the posterior simulated GPP and NEE using the data-conditioned parameters from E0 and E1 experiment. Overall, both experiments can capture the in situ carbon

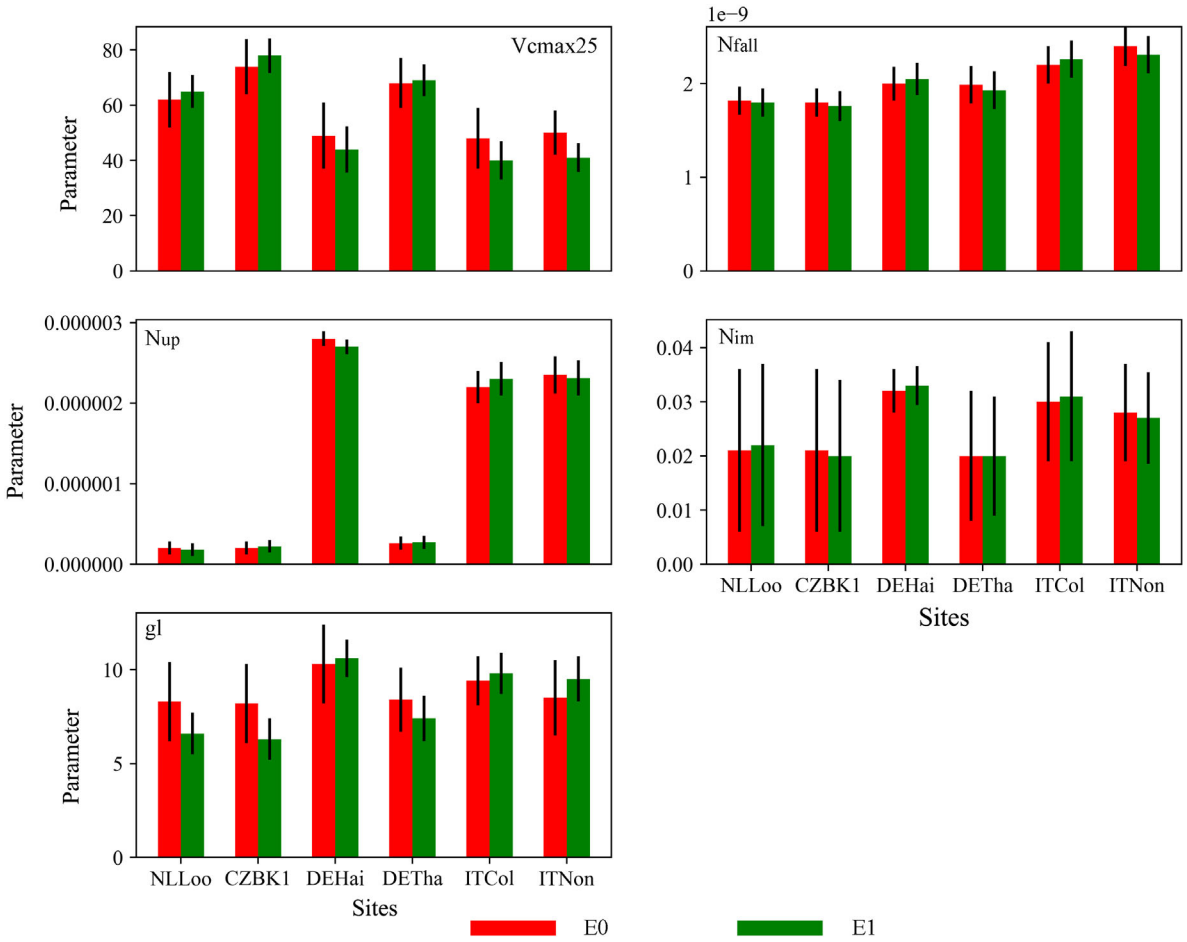

Fig. 1. Comparison of data-conditioned parameters from the two model-data fusion experiments (E0 and E1) at six forest sites. E0 used GPP and NEE observations as constraint, while E1 used GPP, NEE and $\delta^{13}C_f$ observations as constraint. More details on the parameter description in the figure refer to Table 2.

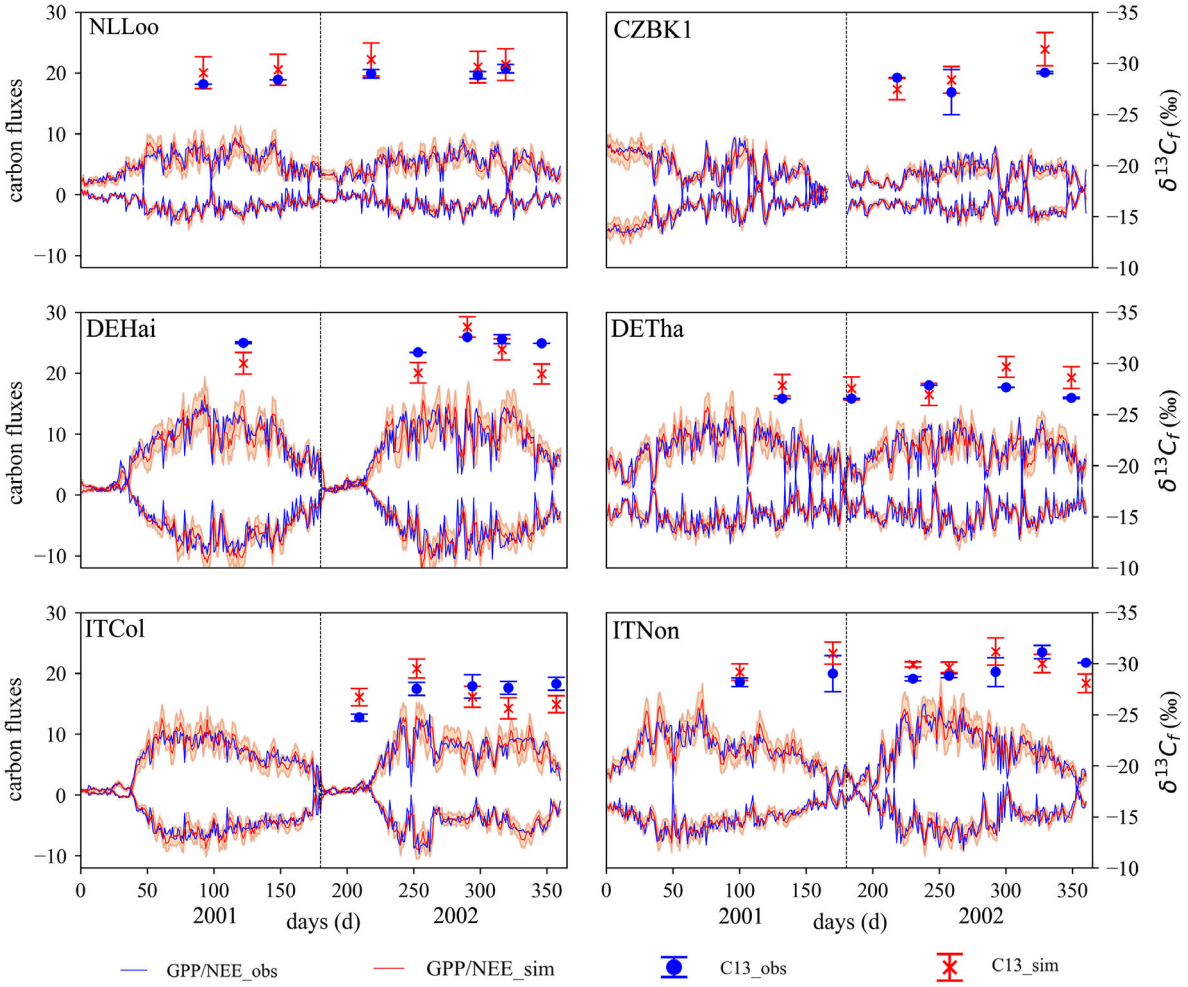

Fig. 2. Comparison between observed (blue) and simulated (red) daily GPP, NEE and $\delta^{13}C_f$ during growing season (May–August) at six forest sites using data-conditioned parameters from E0 experiment. E0 used GPP and NEE observations as constraint.

fluxes variation reasonably well, with the adjusted r^2 ranging from 0.4 to 0.74 (Appendix S1: Fig. S1). However, if only GPP and NEE were assimilated into iTEM (E0 experiment), most $\delta^{13}C_f$ predictions have poor performance against observations during growing season (Fig. 2). When $\delta^{13}C_f$ observation was additionally included into model, the posterior GPP and NEE simulations improved slightly at most sites (Appendix S1: Fig. S1). In addition, the uncertainties of carbon flux predictions were significantly reduced (Appendix S1: Fig. S2, we only showed GPP statistical test here, NEE results were similar). For example, using the parameters from E0 experiment, the daily averaged GPP and NEE values at DE-Tha site were 7.32 ± 0.9 g C/d and −3.32 ± 0.6 g C/d. In comparison, the uncertainties of daily fluxes were reduced to 0.63 and 0.42 g C/d using the conditioned parameters from E1 experiment.

The poorly constrained V_{max25} and $g1$ (larger uncertainties in E0) without the $\delta^{13}C_f$ observations raises the issue of parameter equifinality. Tang and Zhuang (2008, 2009) demonstrated that the terrestrial ecosystem model (TEM) calibrated by using eddy flux tower data was able to reproduce the observed carbon fluxes with very different sets of parameters. Here we also showed that

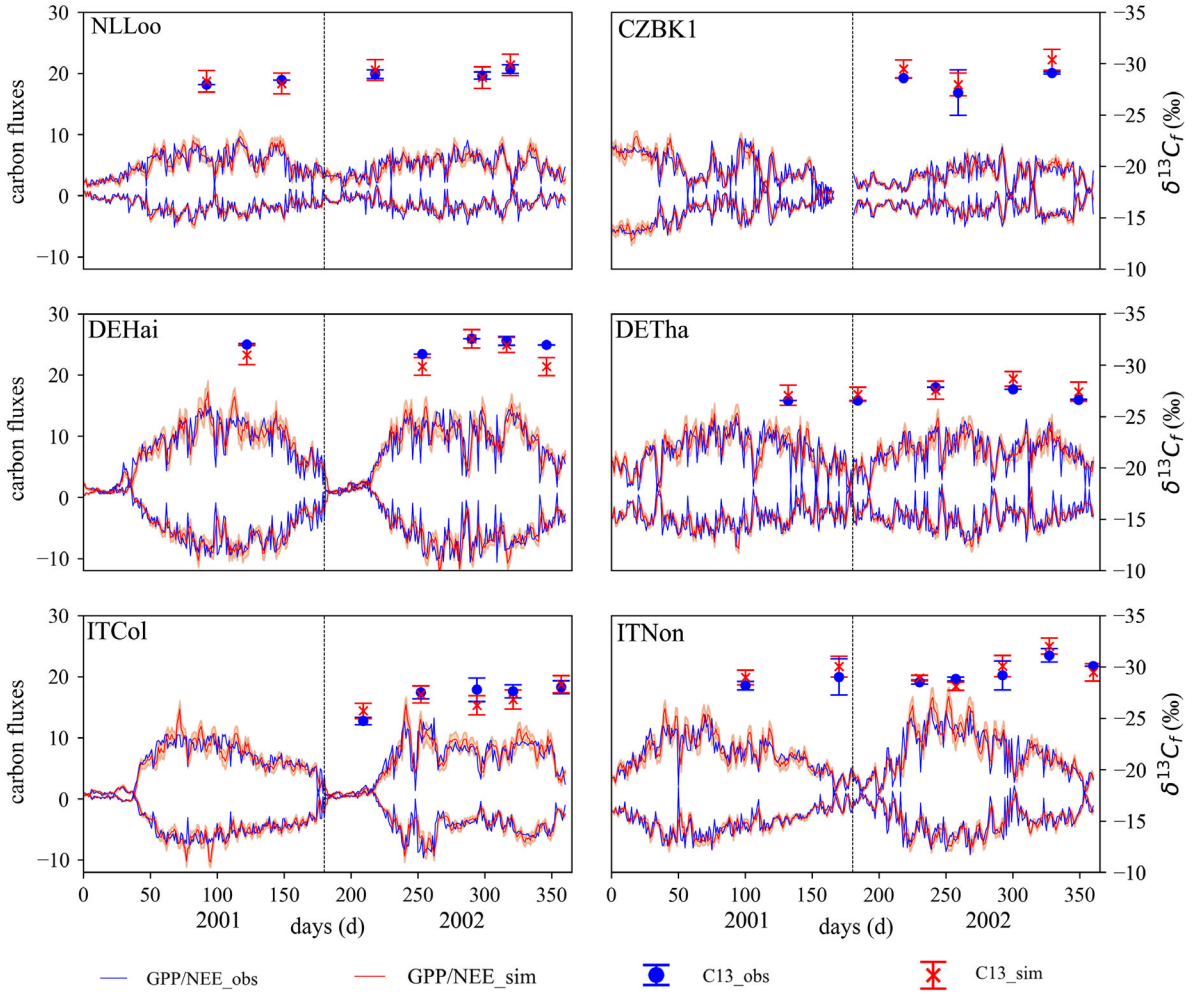

Fig. 3. Comparison between observed (blue) and simulated (red) daily GPP, NEE and $\delta^{13}C_f$ during growing season (May–August) at six forest sites using data-conditioned parameters from E1 experiment. E1 used GPP, NEE, and $\delta^{13}C_f$ observations as constraint.

both model-data fusion experiments had similar results in the posterior carbon fluxes (GPP and NEE) with different V_{max25} and $g1$ values, and however, E0 experiment generated greater uncertainties and large discrepancy existed between the $\delta^{13}C_f$ predictions and observations. This indicated that GPP and NEE data may only have weak constraint on relevant parameters in the coupled stomatal-photosynthesis modules. The leaf $\delta^{13}C$ signal reflects the coupling process between carbon and water fluxes during the photosynthetic activity, enabling these fluxes to be integrated and mutually constrained within the model. These isotopic values are related to both stomatal conductance and canopy photosynthesis, which together determine the CO_2 concentration in the chloroplast (Cc), and consequently the photosynthetic discrimination (Farquhar et al. 1989). Therefore, leaf $\delta^{13}C$ can shed light on physiological responses to environmental conditions such as drought, temperature, and relative humidity (Williams et al. 2010, Voelker et al. 2014, Hartl-Meier et al. 2015) and provides useful constraint on the photosynthetic and stomatal conductance-related parameters (V_{max25} and $g1$ in our study). Our model-data fusion results at multiple forest sites were consistent with other studies (Aranibar et al. 2006; Duarte et al. 2017),

which also confirmed that relevant photosynthetic parameters can be further constrained by using isotopic signal of leaves. We further found that the modeled canopy conductance in E1 parameterization schemes showed better performance against observation than that in E0 experiment (Appendix S1: Table S1), indicating that the calibrated iTEM in the E1 experiment may better capture the observed response of canopy conductance to environmental change (e.g., vapor pressure deficit).

The slope of stomatal model (g1)

By assimilating the $\delta^{13}C_f$ observation (E1 experiment), we found $g1$ to be spatially variable among the six sites and there was a significantly positive relationship between the $g1$ estimates and annual precipitation (Fig. 4), indicating that the stomatal conductance of temperate forest is more sensitive under favorable environment. Previous observations reported a large variation in $g1$ values among plant function types (PFTs) and even within similar or same species (Baldocchi and Meyers 1998; Lin et al. 2015; Miner et al. 2017) and this variation was generally found to increase with growth temperature and soil water availability (Bauerle et al. 2003; Lin et al. 2015). As for the water availability effect on $g1$, vegetation in less humid region generally has specific structural issues that can endure unfavorable periods (Hacke and Sperry 2001). Such tissue requires large investment of carbon (Wright et al. 2003), resulting in more conservative stomatal behaviors and more efficient water use (Cowan and Farquhar 1977). The reduction of parameterized $g1$ in Ball-Berry model may help to reduce water loss in hot and dry environment in water-limited regions, suggesting a limitation of carbon assimilation by water availability. Based on the long-standing theory of optimal photosynthesis-stomatal process, Medlyn et al. (2011) proposed a tractable stomatal model, which is functionally equivalent to the widely used empirical stomatal model (e.g., Ball-Berry model). Based on Medlyn's model, Lin et al. (2015) compiled a global database of stomatal conductance from a wide range of field studies and they found that marginal water costs of carbon uptake (similar term

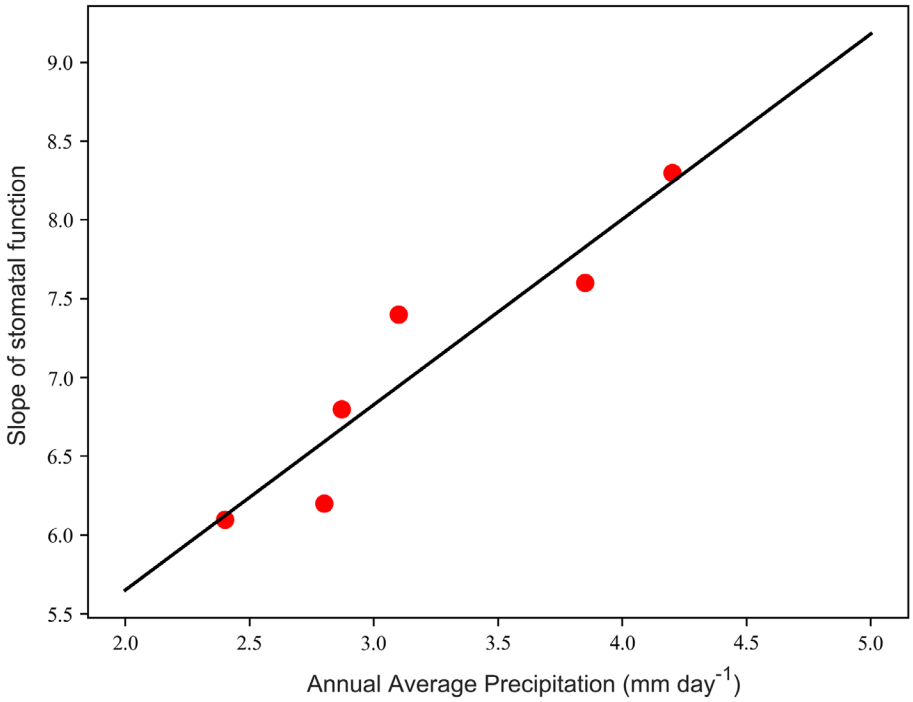

Fig. 4. Statistical relationship between annual precipitation and the slope of stomatal model derived from the E1 experiment among the six forest sites.

with $g1$ in Ball-Berry model) was lower in water-limited regions, which is consistent with our model-data fusion results, indicating the wetter site had larger $g1$ estimation. No significant statistical relationship is found between $g1$ and other climate variables (Fig. S3), while Lin et al. (2015) demonstrated that $g1$ increased with temperature. It is possible that our model-data fusion experiments were based on only six sites, which may not capture the relationship across a wide range of climate gradients. In addition, the global database of stomatal conductance was derived from leaf scale gas measurement, while the iTEM model uses a big-leaf model, indicating the parameterized $g1$ actually represents the averaged properties of the whole canopy.

We further showed that there was a spatial variability in this constraint on model parameters. For example, using the final data-conditioned $g1$ parameter (Fig. 3, E1 experiment) at the DETha site for simulations at other five sites resulted in large deviations from the observed annual mean $\delta^{13}C_f$ (Appendix S1: Fig. S4). This suggested that the single site-level derived parameter may not be valid for other sites and the spatially variable $g1$ should be considered for accurately simulating $\delta^{13}C_f$. Although $g1$ can greatly impact on transpiration and carbon fluxes (Leuning et al. 1998; Luo et al. 2001; Barnard and Bauerle 2013; Bauerle et al. 2014), current earth system models assume it to be spatially constant (e.g., in the Community Land Model 4.5, $g1$ is 9.0 in deciduous forest) without considering its possible change resulting from the plant adaption to climate gradient. De Kauwe et al. (2015) first attempted to represent the spatially variable $g1$ parameter in a land surface model based on plant functional types (PFTs) and environmental conditions. They found that the $g1$ variability greatly affected annual fluxes of transpiration across evergreen needleleaf forest, tundra and C4 grass regions. Here, using the $g1$ parameter estimates conditioned on both carbon fluxes and isotopic signals (E1 experiment) at the six sites, we incorporated the statistical relationship between $g1$ and annual precipitation into iTEM and conducted the regional simulation for temperate forest in the Northern Hemisphere (here we refer as E1-R1). We compared the simulation with results using the parameters derived from E0 experiment (E0-R0). Since no significant relationships were found between the other four parameter estimates and environmental conditions, we simply used the averaged estimates in each PFT (DBF and ENF). Thus, in both regional simulations, only $g1$ was precipitation dependent in E1-R1, while other parameters were spatially constant within one PFT. It should be noted that a number of studies found that $g1$ can vary seasonally, in response to soil water availability (Tenhunen et al. 1990; Misson et al. 2004), light (Bunce 1998; Aasamaa and Sõber 2011), and elevated CO_2 (Kellomaki and Wang 1997; Tausz-Posch et al. 2013). The temporal variations have been reported in trees (Falge et al. 1996; Misson et al. 2004; Barnard and Bauerle 2013; Gimeno et al. 2016) and crops (Leakey et al. 2006; Miner et al. 2017). However, other observations show contradictory results (Xu and Baldocchi 2003; Weber and Gates 1990; Liozon et al. 2000; Medlyn et al. 2001) and the extent to which $g1$ change is still debated. Therefore, the impacts of potential $g1$ seasonal changes are not considered here.

Regional simulations

Both simulations (E0-R0 and E1-R1) can well capture the spatial GPP and NEP variability across the temperate forest region in the North Hemisphere (Figs. 5, 6). The Gulf Coast and parts of the Southeast US were the most productive regions, with GPP around 2000 g $C{\cdot}m^{-2}{\cdot}yr^{-1}$ and NEP greater than 500 g $C{\cdot}m^{-2}{\cdot}yr^{-1}$, while the North China and Tibet-Plateau generally had relatively low GPP (500 g $C{\cdot}m^{-2}{\cdot}yr^{-1}$) and NEP (100 g $C{\cdot}m^{-2}{\cdot}yr^{-1}$). The comparison between the two simulations showed that E0-R0 was predicted to be slightly higher than E1-R1, with the GPP difference ranging from 50 to 150 g $C{\cdot}m^{-2}{\cdot}yr^{-1}$ and NEP difference from 50 to 100 g $C{\cdot}m^{-2}{\cdot}yr^{-1}$, respectively. Larger differences were observed in the regions characterized by high productivity, such as the Southeast US and East China. We further evaluated the regional simulations with a data-driven product-Fluxcom (http://www.fluxcom.org). The Fluxcom dataset includes energy and carbon flux predictions which were upscaled to the globe based on machine learning methods that integrate FLUXNET site-level observations, satellite remote sensing, and meteorological data (Jung et al. 2019). From 2003 to 2010, the spatiotemporally

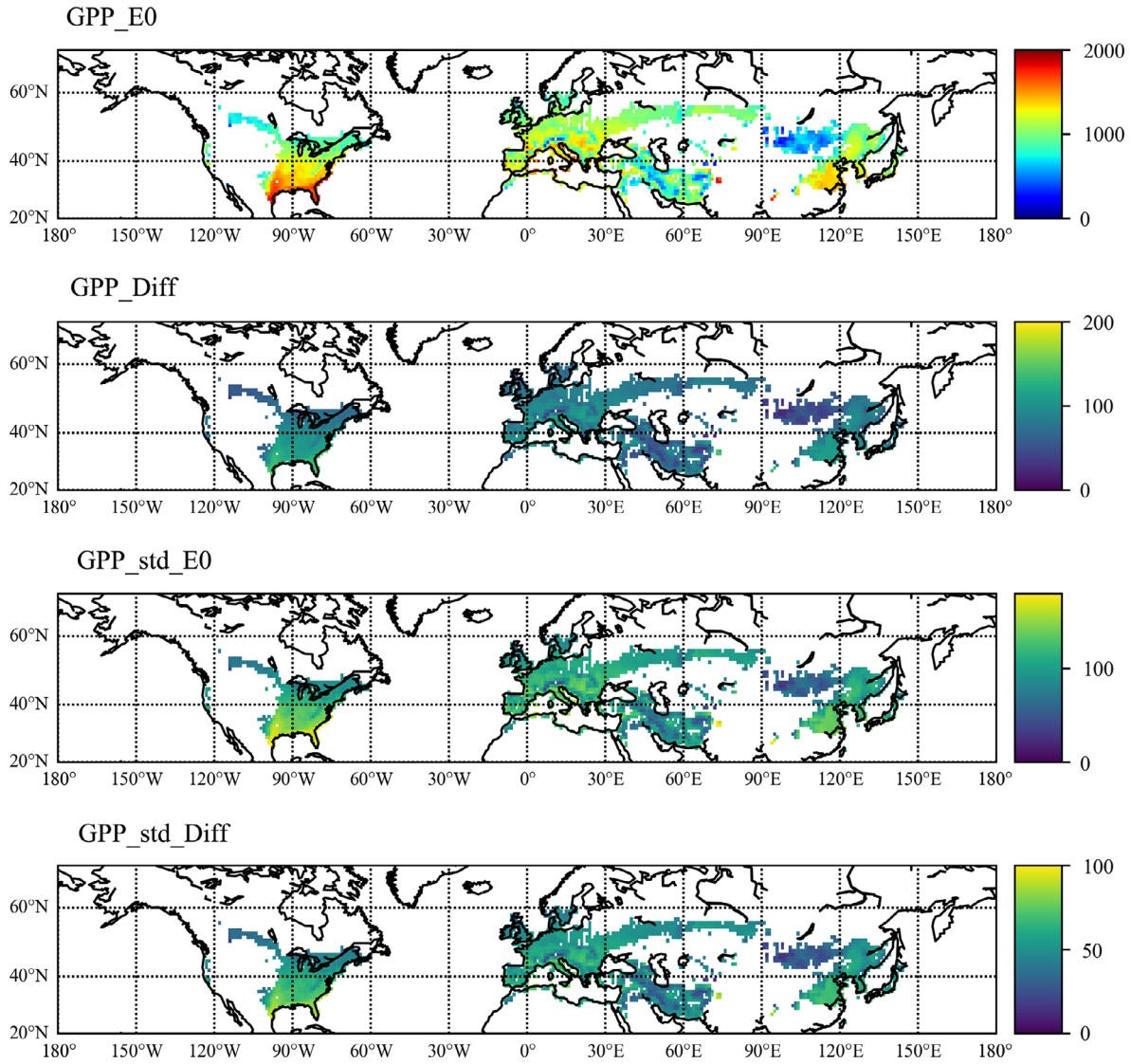

Fig. 5. GPP estimation and its uncertainty (stand deviation-std) by E0-R0 simulation in temperate forest regions of the Northern Hemisphere. The differences (_Diff) of GPP and its uncertainty are calculated as E0-R0 minus E1-R1. E0-R0 and E1-R1 stand for the regional simulations using parameters from the E0 and E1 model-data fusion experiment, respectively (Units: g $C{\cdot}m^{-2}{\cdot}yr^{-1}$).

averaged GPP and NEP in Fluxcom in the study region were 1047 and 534 g $C{\cdot}m^{-2}{\cdot}yr^{-1}$, which was comparable with the results in E0-R0 (GPP: 1240 g $C{\cdot}m^{-2}{\cdot}yr^{-1}$; NEP: 495 g $C{\cdot}m^{-2}{\cdot}yr^{-1}$) and E1-R1 (GPP: 1123 g $C{\cdot}m^{-2}{\cdot}yr^{-1;}$ NEP: 465 g $C{\cdot}m^{-2}{\cdot}yr^{-1}$). However, the parameter estimates from the E0 experiment performed worse than those from E1 experiment in reproducing the annual GPP and NEP from Fluxcom (Appendix S1: Fig. S5). This indicated that the conditioned model parameters with additional $\delta^{13}C_f$ measurement better constrain regional carbon fluxes.

We further found that the uncertainties of estimated GPP and NEP were larger in the simulations without the $\delta^{13}C_f$ constraint (E0-R0), and the spatial differences were obvious in high productivity areas (Figs. 5, 6). For example, the standard deviation of GPP was around 150 g

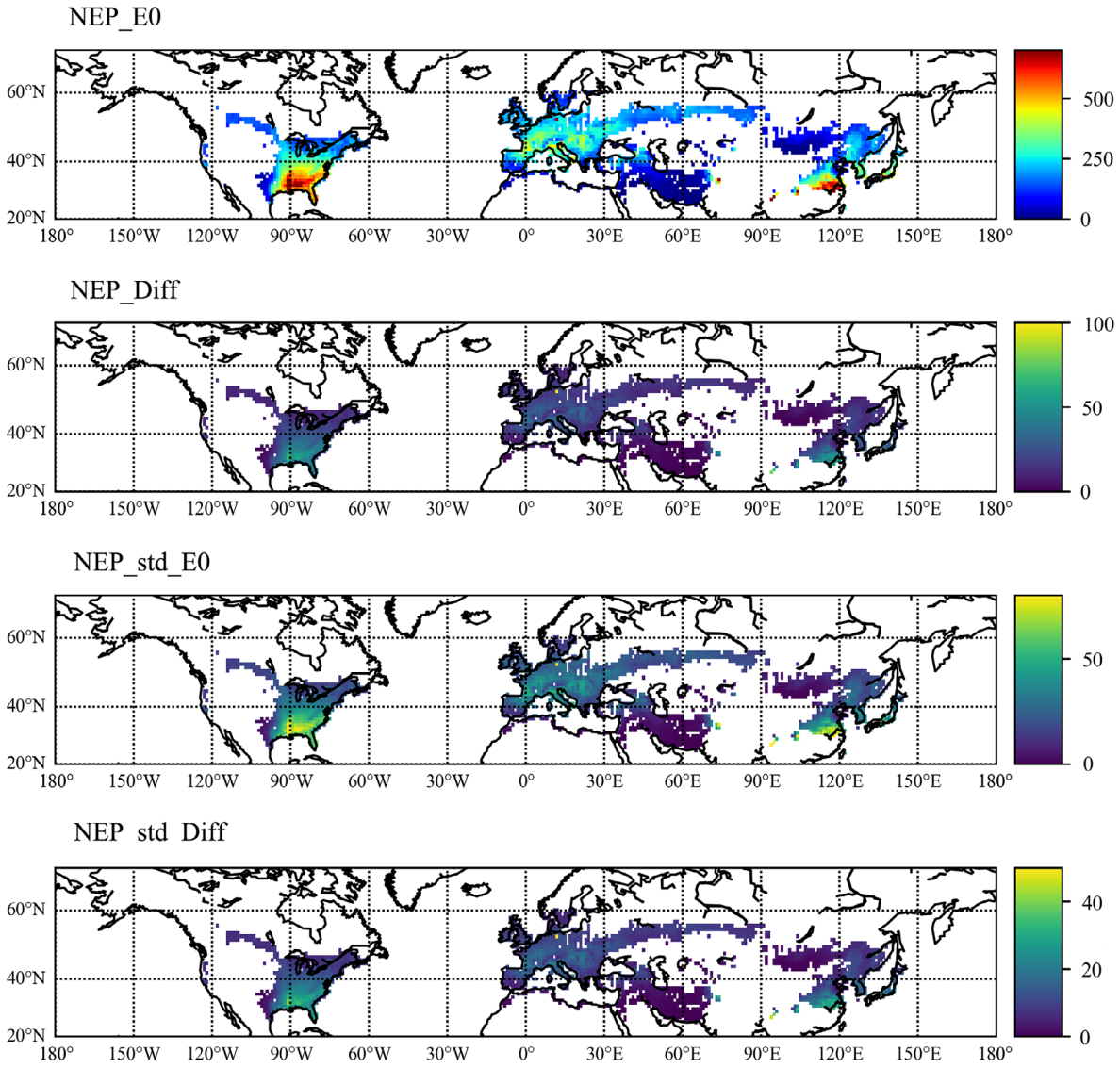

Fig. 6. NEP estimation and its uncertainty (stand deviation-std) by E0-R0 simulation in temperate forest regions of the Northern Hemisphere. The differences (_Diff) of NEP and its uncertainty are calculated as E0-R0 minus E1-R1. E0-R0 and E1-R1 stand for the regional simulations using parameters from the E0 and E1 model-data fusion experiment, respectively (Units: g $C \cdot m^{-2} \cdot yr^{-1}$).

$C \cdot m^{-2} \cdot yr^{-1}$ in the Southeast US in E0 and in E1, around 120 g $C \cdot m^{-2} \cdot yr^{-1}$. The uncertainty induced by the wide parameters space also exhibited a strong seasonal variation (Appendix S1: Fig. S6). For both E0-R0 and E1-R1, the GPP and NEP uncertainty was larger in summer season (from June to August), but small in winter (from November to January). This was consistent with the site-level calibration and validation (Fig. 3), which showed a relatively larger uncertainty in growing season (non-growing season is not presented here). It was also noted that the GPP and NEP uncertainties had the most reduction in summer season when iTEM used additional $\delta^{13}C_f$ constraints. For example, the summer GPP uncertainty in the Southeast US was reduced by 25%, from 40 to 30 g $C \cdot m^{-2} \cdot month^{-1}$ (Appendix S1: Fig. S3).

Implication and limitation

By implementing a rigorous model-data fusion approach at multiple forest sites, our results confirmed that in situ $\delta^{13}C_f$ measurement can consistently constrain LSM parameters and carbon flux uncertainties, implying that $\delta^{13}C_f$ observations may help improve model parameterization at other sites with different climate or species. Furthermore, the significant relationship between $g1$ and climate gradient was found in the experiment that includes $\delta^{13}C_f$ constraints.

Our model-data fusion also demonstrated that the spatially variable $g1$ was essential for accurately predicting site-level $\delta^{13}C_f$, challenging the current modeling paradigm that vegetation parameters share the same values within one PFT. Recent studies began to explore statistical methods (Verheijen et al. 2015; Butler et al. 2017) or probabilistic approach (Wang et al. 2009; Pappas et al. 2016) to explicitly incorporate the spatial variation into ESMs based on the global trait database (TRY) (Kattge et al. 2011). Although these studies present important advances in representing spatially variable parameters, they failed to consider the uncertainties of the sparse database and the derived correlation between vegetation parameters and climate is generally weak for spatial extrapolations (Wright et al. 2005; Ordoñez et al. 2009; Coyle et al. 2014). By comparison, our data fusion approach can effectively constrain model parameters by maximizing the use of in situ observation and remote sensing data with different sources and spatiotemporal resolutions. This allows us to efficiently build the statistical relationship between the data-conditioned parameters and biotic and abiotic factors. Future efforts should also focus on identifying the potential temporal variation in plant parameters (Williams et al. 2009; Liu and Ng 2019) based on more plant trait data.

A few limitations need to be addressed in the future. First, simply assuming that the mesophyll conductance is proportional to the Rubisco content (Evans and von Caemmerer 1996) may bias our predicted carbon fluxes. Leaf gas-exchange measurements suggest that the mesophyll conductance varies with leaf development (Warren 2008), nutrient availability (Warren 2004), radiation (Grassi and Magnani 2005, Niinemets et al. 2006), and leaf temperature (Bernacchi et al. 2002). Although previous studies empirically described the mesophyll conductance as a function of plant physiological traits and climate variability (Suits et al. 2005, Sun et al. 2014), the understanding of the response of mesophyll conductance to environmental conditions is still limited (Bodin et al. 2013). Second, the effect of soil moisture on stomatal conductance is not considered here, which may affect the predictability of plant responses under drought conditions. Soil water stress and vapor pressure deficit can occur simultaneously, and however, the underlying mechanistic or physiological knowledge of the interaction between soil water availability and stoma is often difficult to be modeled (Damour et al. 2010). In addition, plant morphology often changes under water shortage condition (e.g., the increase root to shoot ratio), and these adaptive strategies could in turn attenuate the negative effects on stomatal conductance. Whether stomatal (soil water shortage directly influences the stomatal closure) or non-stomatal (soil water shortage influences the photosynthetic capacity or mesophyll conductance) limitation dominates the carbon flux is still debated (Egea et al. 2010; Keenan et al. 2010, Kauwe et al. 2015), in particular concerning the response at different time scales. Both experiment which links stomatal function to plant traits and environmental variables and theoretical studies would help understand the physiology of observed stomatal behavior, which can be integrated into future modeling studies.

Conclusion

Land surface models usually consist of multiple computational modules integrating biological, hydrological, and physical processes and a group of parameters associated with these processes and controls. Carbon isotope discrimination by terrestrial ecosystems, which is affected by variable environmental conditions (e.g., air humidity, temperature, and light), have the potential to further constrain model parameters. Here we incorporated photosynthetic carbon isotope discrimination data into a process-based ecosystem model (iTEM) using an Ensemble Kalman Filter (EnKF) to constrain model parameters at six temperate forest sites. The carbon flux observations with and without $\delta^{13}C_f$ measurements were used. When only carbon flux observations

were assimilated into iTEM, a wide range of parameter values were found to be able to capture in situ observation, resulting in large deviations from $\delta^{13}C_f$ observations and great uncertainties in the posterior carbon fluxes. In contrast, including $\delta^{13}C_f$ measurements can narrow the estimated ranges of maximum carboxylation rate at 25°C (V_{cmax25}) and slope of stomatal conductance ($g1$) and reduce the simulated carbon flux uncertainties. We further found that when $\delta^{13}C_f$ was used as constraint, the $g1$ parameter estimates co-varied with annual precipitation among the six forest sites, and its spatial variation was essential for accurately predicting site-level $\delta^{13}C_f$. The comparison of regional simulations using the parameter sets from the two model-data fusion experiments showed that including $\delta^{13}C_f$ measurement led to slightly better performance against the FLUXCOM products and less uncertainties in the carbon flux predictions. Our model-data fusion study at multiple forest sites demonstrated the potential of using $\delta^{13}C_f$ to constrain carbon flux uncertainties.

Acknowledgments

This study is supported through funded projects to Q. Z. by the NASA Land-Use and Land-Cover Change program (NASANNX09AI26G), Department of Energy (DE-FG02-08ER64599), the NSF Division of Information and Intelligent Systems (NSF-1028291), and the NSF Carbon and Water in the Earth Program (NSF-0630319). The supercomputing resource is provided by the Rosen Center for Advanced Computing at Purdue University.

Literature Cited

Aasamaa, K., and A. Sõber. 2011. Stomatal sensitivities to changes in leaf water potential, air humidity, CO_2 concentration and light intensity, and the effect of abscisic acid on the sensitivities in six temperate deciduous tree species. Environmental and Experimental Botany 71:72–78.

Aranibar, J. N., J. A. Berry, W. J. Riley, D. E. Pataki, B. E. Law, and J. R. Ehleringer. 2006. Combining meteorology, eddy fluxes, isotope measurements, and modeling to understand environmental controls of carbon isotope discrimination at the canopy scale. Global Change Biology 12:710–730.

Arens, N. C., A. H. Jahren, and R. Amundson. 2000. Can C3 plants faithfully record the carbon isotopic composition of atmospheric carbon dioxide? Paleobiology 26:137–164.

Baldocchi, D., and T. Meyers. 1998. On using ecophysiological, micrometeorological and biogeochemical theory to evaluate carbon dioxide, water vapor and trace gas fluxes over vegetation: a perspective. Agricultural and Forest Meteorology 90:1–25.

Bauerle, W. L., T. H. Whitlow, T. L. Setter, T. L. Bauerle, and F. M. Vermeylen. 2003. Ecophysiology of Acer rubrum seedlings from contrasting hydrologic habitats: growth, gas exchange, tissue water relations, abscisic acid and carbon isotope discrimination. Tree Physiology 23:841–850.

Bauerle, W. L., A. B. Daniels, and D. M. Barnard. 2014. Carbon and water flux responses to physiology by environment interactions: a sensitivity analysis of variation in climate on photosynthetic and stomatal parameters. Climate Dynamics 42:2539–2554.

Barnard, D. M., and W. L. Bauerle. 2013. The implications of minimum stomatal conductance on modeling water flux in forest canopies. Journal of Geophysical Research: Biogeosciences 118:1322–1333.

Bernacchi, C. J., A. R. Portis, H. Nakano, S. von Caemmerer, and S. P. Long. 2002. Temperature response of mesophyll conductance. Implications for the determination of rubisco enzyme kinetics and for limitations to photosynthesis in vivo. Plant Physiology 130:1992–1998.

Bernhofer, C. 2003. Spruce forests (Norway and Sitka Spruce, Including Douglas Fir): Carbon and water fluxes and balances, ecological and ecophysiological determinants. Fluxes of Carbon, Water and Energy of European Forests 163:99–123.

Bodin, P. E., et al. 2013. Comparing the performance of different stomatal conductance models using modelled and measured plant carbon isotope ratios (δ13C): implications for assessing physiological forcing. Global Change Biology 19:1709–1719.

Bowling, D. R., N. G. McDowell, B. J. Bond, B. E. Law, and J. R. Ehleringer. 2002. 13C content of ecosystem respiration is linked to precipitation and vapor pressure deficit. Oecologia 131:113–124.

Bowling, D. R., P. P. Tans, and R. K. Monson. 2001. Partitioning net ecosystem carbon exchange with isotopic fluxes of CO_2. Global Change Biology 7:127–145.

Brüggemann, N., et al. 2011. Carbon allocation and carbon isotope fluxes in the plant-soil-atmosphere continuum: a review. Biogeosciences 8:3457–3489.

Bunce, J. A. 1998. Effects of humidity on short-term responses of stomatal conductance to an increase in carbon dioxide concentration. Plant, Cell and

Environment 21:115–120. https://doi.org/10.1046/j.1365-3040.1998.00253.x.

Butler, E. E., et al., 2017. Mapping local and global variability in plant trait distributions. Proceedings of the National Academy of Sciences USA 114(51): E10937–E10946.

Chen, M. 2013. Evaluation of atmospheric aerosol and tropospheric ozone effects on global terrestrial ecosystem carbon dynamics. ProQuest Dissertations and Theses.

Chen, M., and Q. Zhuang. 2014. Evaluating aerosol direct radiative effects on global terrestrial ecosystem carbon dynamics from 2003 to 2010. Tellus B: Chemical and Physical Meteorology 66:21808.

Ciais, P., P. P. Tans, J. W. C. White, M. Trolier, R. J. Francey, J. A. Berry, D. R. Randall, P. J. Sellers, J. G. Collatz, and D. S. Schimel. 1995. Partitioning of ocean and land uptake of CO_2 as inferred by δ13C measurements from the NOAA Climate Monitoring and Diagnostics Laboratory Global Air Sampling Network. Journal of Geophysical Research 100:5051.

Cowan, I. R., and G. D. Farquhar 1977. Stomatal function in relation to leaf metabolism and environment. Integration of activity in the higher plant. Pages 471–505. Cambridge University Press, Cambridge, UK.

Coyle, J. R., F. W. Halliday, B. E. Lopez, K. A. Palmquist, P. A. Wilfahrt, and A. H. Hurlbert. 2014. Using trait and phylogenetic diversity to evaluate the generality of the stress-dominance hypothesis in eastern North American tree communities. Ecography 37:814–826.

Dai, Y., R. E. Dickinson, and Y.-P. Wang. 2004. A two-big-leaf model for canopy temperature, photosynthesis, and stomatal conductance. Journal of Climate 17:2281–2299.

Damour, G., T. Simonneau, H. Cochard, and L. Urban. 2010. An overview of models of stomatal conductance at the leaf level. Plant, Cell and Environment 33:1419–1438.

De Kauwe, M. G., J. Kala, Y.-S. Lin, A. J. Pitman, B. E. Medlyn, R. A. Duursma, G. Abramowitz, Y.-P. Wang, and D. G. Miralles. 2015. A test of an optimal stomatal conductance scheme within the CABLE land surface model. Geoscientific Model Development 8:431–452.

Diefendorf, A. F., K. E. Mueller, S. L. Wing, P. L. Koch, and K. H. Freeman. 2010. Global patterns in leaf 13C discrimination and implications for studies of past and future climate. Proceedings of the National Academy of Sciences of the United States of America 107:5738–5743.

Dolman, A. J., E. J. Moors, and J. A. Elbers. 2002. The carbon uptake of a mid latitude pine forest growing on sandy soil. Agricultural and Forest Meteorology 111:157–170.

Duarte, H. F., B. M. Raczka, D. M. Ricciuto, J. C. Lin, C. D. Koven, P. E. Thornton, D. R. Bowling, L. Chun-Ta, K. J. Bible, and J. R. Ehleringer. 2017. Evaluating the Community Land Model (CLM4.5) at a coniferous forest site in northwestern United States using flux and carbon-isotope measurements. Biogeosciences 14:4315–4340.

Egea, G., A. Verhoef, and P. L. Vidale. 2011. Towards an improved and more flexible representation of water stress in coupled photosynthesis–stomatal conductance models. Agricultural & Forest Meteorology 151:1370–1384.

Evans, J. R., and S. Von Caemmerer. 1996. Carbon dioxide diffusion inside leaves. Plant Physiology 110:339–346.

Evensen, G. 1994. Sequential data assimilation with a nonlinear quasi-geostrophic model using Monte Carlo methods to forecast error statistics. Journal of Geophysical Research 99(C5):10143.

Evensen, G. 2009. Data assimilation: The ensemble Kalman filter. Springer, Berlin, Germany.

Falge, E., W. Graber, R. Siegwolf, and J. D. Tenhunen. 1996. A model of the gas exchange response of *Picea abies* to habitat conditions. Trees 10:277–287.

Farquhar, G. D., and R. A. Richards. 1984. Isotopic composition of plant carbon correlates with water-use efficiency of wheat genotypes. Functional Plant Biology 11:539–552.

Farquhar, G. D., S. von Caemmerer, and J. A. Berry. 1980. A biochemical model of photosynthetic CO_2 assimilation in leaves of C3 species. Planta 149:78–90.

Farquhar, G. D., J. R. Ehleringer, and K. T. Hubick. 1989. Carbon isotope discrimination and photosynthesis. Annual Review of Plant Physiology and Plant Molecular Biology 40(1):503–537.

Fung, I., et al. 1997. Carbon 13 exchanges between the atmosphere and biosphere. Global Biogeochemical Cycles 11:507–533.

Gimeno, T. E., K. Y. Crous, C. Julia, A. P. O'Grady, Ó. Anna, B. E. Medlyn, and D. S. Ellsworth. 2016. Conserved stomatal behaviour under elevated CO_2 and varying water availability in a mature woodland. Functional Ecology 30:700–709.

Grassi, G., and F. Magnani. 2005. Stomatal, mesophyll conductance and biochemical limitations to photosynthesis as affected by drought and leaf ontogeny in ash and oak trees. Plant, Cell and Environment 28:834–849.

Griffis, T. J., J. M. Baker, S. D. Sargent, M. Erickson, J. Corcoran, M. Chen, and K. Billmark. 2010. Influence of C4 vegetation on $13CO_2$ discrimination and

isoforcing in the upper Midwest, United States. Global Biogeochemical Cycles 24:GB4006.

Hacke, U. G., and J. S. Sperry. 2001. Functional and ecological xylem anatomy. Perspectives in Plant Ecology, Evolution and Systematics 4:97–115.

Hartl-Meier, C., C. Zang, U. Buntgen, J. Esper, A. Rothe, A. Gottlein, T. Dirnbock, and K. Treydte. 2015. Uniform climate sensitivity in tree-ring stable isotopes across species and sites in a mid-latitude temperate forest. Tree Physiology 35:4–15.

Intergovernmental Panel on Climate Change (IPCC). 2014. Climate Change 2013: The Physical Science Basis. Pages 1–32 *in* Contribution of Working Group I to the Fifth Assessment Report of the Intergovernmental Panel on Climate Change. Cambridge University Press, Cambridge, UK.

Jung, M., S. Koirala, U. Weber, K. Ichii, F. Gans, G. Camps-Valls, D. Papale, C. Schwalm, G. Tramontana, and M. Reichstein. 2019. The FLUXCOM ensemble of global land-atmosphere energy fluxes. Scientific Data, 6:74.

Kaplan, J. O., I. C. Prentice, and N. Buchmann. 2002. The stable carbon isotope composition of the terrestrial biosphere: Modeling at scales from the leaf to the globe. Global Biogeochemical Cycles 16:8–11.

Kattge, J., et al. 2011. TRY - a global database of plant traits. Global Change Biology, 17:2905–2935.

Keenan, T., S. Sabate, and C. Gracia. 2010. The importance of mesophyll conductance in regulating forest ecosystem productivity during drought periods. Global Change Biology 16:1019–1034.

Kellomaki, S., and K.-Y. Wang 1997. Effects of elevated O_3 and CO_2 concentrations on photosynthesis and stomatal conductance in Scots pine. Plant, Cell and Environment 20:995–1006.

Knohl, A., E.-D. Schulze, O. Kolle, and N. Buchmann. 2003. Large carbon uptake by an unmanaged 250-year-old deciduous forest in Central Germany. Agricultural and Forest Meteorology 118:151–167.

Leakey, A. D. B., C. J. Bernacchi, D. R. Ort, and S. P. Long. 2006. Long-term growth of soybean at elevated [CO_2] does not cause acclimation of stomatal conductance under fully open-air conditions. Plant, Cell and Environment 29(9):1794–1800. https://doi.org/10.1111/j.1365-3040.2006.01556.x.

Leuning, R., F. X. Dunin, and Y.-P. Wang. 1998. A two-leaf model for canopy conductance, photosynthesis and partitioning of available energy. II. Comparison with measurements. Agricultural and Forest Meteorology 91:113–125.

Liozon, R., F.-W. Badeck, B. Genty, S. Meyer, and B. Saugier. 2000. Leaf photosynthetic characteristics of beech (*Fagus sylvatica*) saplings during three years of exposure to elevated CO2 concentration. Tree Physiology 20:239–247.

Lin, Y.-S., et al. 2015. Optimal stomatal behaviour around the world. Nature Climate Change 5:459–464.

Liu, S., M. Chen, and Q. Zhuang. 2014. Aerosol effects on global land surface energy fluxes during 2003–2010. Geophysical Research Letters 41:7875–7881.

Liu, S., and G. H. C. Ng. 2019. A data-conditioned stochastic parameterization of temporal plant trait variability in an ecohydrological model and the potential for plasticity. Agricultural and Forest Meteorology 274:184–194.

Liu, S., Q. Zhuang, M. Chen, and L. Gu. 2016. Quantifying spatially and temporally explicit CO2 fertilization effects on global terrestrial ecosystem carbon dynamics. Ecosphere 7:e01391. https://doi.org/10.1002/ecs2.1391.

Luo, Y., B. Medlyn, D. Hui, D. Ellsworth, J. Reynolds, and G. Katul. 2001. Gross primary productivity in duke forest: modeling synthesis of CO2 experiment and eddy–flux data. Ecological Applications, 11:239–252.

Marshall, J. D., J. R. Brooks, and K. Lajtha. 2007. Sources of variation in the stable isotopic composition of plants. Pages 22–60. Stable isotopes in ecology and environmental science. Blackwell Publishing Ltd., Boston, Massachusetts, USA.

Medlyn, B. E., R. A. Duursma, D. Eamus, D. S. Ellsworth, I. C. Prentice, C. V. M. Barton, K. Y. Crous, P. De Angelis, M. Freeman, and L. Wingate. 2011. Reconciling the optimal and empirical approaches to modelling stomatal conductance. Global Change Biology 17:2134–2144.

Medlyn, B. E., et al. 2001. Stomatal conductance of forest species after long-term exposure to elevated CO_2 concentration: a synthesis. New Phytologist 149:247–264.

Miner, G. L., W. L. Bauerle, and D. D. Baldocchi. 2017. Estimating the sensitivity of stomatal conductance to photosynthesis: a review. Plant, Cell & Environment 40:1214–1238.

Misson, L., J. A. Panek, and A. H. Goldstein. 2004. A comparison of three approaches to modeling leaf gas exchange in annually drought-stressed ponderosa pine forests. Tree Physiology 24:529–541.

Niinemets, Ü. L. O., A. Cescatti, M. Rodeghiero, and T. Tosens. 2006. Complex adjustments of photosynthetic potentials and internal diffusion conductance to current and previous light availabilities and leaf age in Mediterranean evergreen species *Quercus ilex*. Plant, Cell and Environment 29:1159–1178.

Ordoñez, J. C., M. van Bodegom Peter, J.-P. Witte, I. J. Wright, P. B. Reich, and A. Rien. 2009. A global study of relationships between leaf traits, climate

and soil measures of nutrient fertility. Global Ecology and Biogeography 18:137–149.

Pappas, C., S. Fatichi, and P. Burlando. 2016. Modeling terrestrial carbon and water dynamics across climatic gradients: does plant trait diversity matter? New Phytologist 209:137–151.

Raczka, B., H. F. Duarte, C. D. Koven, D. Ricciuto, P. E. Thornton, J. C. Lin, and D. R. Bowling. 2016. An observational constraint on stomatal function in forests: evaluating coupled carbon and water vapor exchange with carbon isotopes in the Community Land Model (CLM4. 5). 5183–5204.

Rebmann, C., et al. 2005. Quality analysis applied on eddy covariance measurements at complex forest sites using footprint modelling. Theoretical and Applied Climatology 80:121–141.

Reichstein, M., et al. 2005. On the separation of net ecosystem exchange into assimilation and ecosystem respiration: review and improved algorithm. Global Change Biology 11:1424–1439.

Sage, R. F. 1999. 1 - Why C4 photosynthesis? C4 plant biology. Pages 3–16 *in* Physiological ecology. Academic Press, San Diego, California¸ USA.

Saurer, M., R. T. W. Siegwolf, and F. H. Schweingruber. 2004. Carbon isotope discrimination indicates improving water-use efficiency of trees in northern Eurasia over the last 100 years. Global Change Biology 10:2109–2120.

Scholze, M., P. Ciais, and M. Heimann. 2008. Modeling terrestrial 13C cycling: Climate, land use and fire. Global Biogeochemical Cycles 22:n/a–n/a.

Seibt, U., A. Rajabi, H. Griffiths, and J. A. Berry. 2008. Carbon isotopes and water use efficiency: Sense and sensitivity. Oecologia 155:441–454.

Suits, N. S., A. S. Denning, J. A. Berry, C. J. Still, J. Kaduk, J. B. Miller, and I. T. Baker. 2005. Simulation of carbon isotope discrimination of the terrestrial biosphere. Global Biogeochemical Cycles 19:n/a–n/a.

Sun, Y., L. Gu, R. E. Dickinson, R. J. Norby, S. G. Pallardy, and F. M. Hoffman. 2014. Impact of mesophyll diffusion on estimated global land CO_2 fertilization. Proceedings of the National Academy of Sciences of the United States of America 111:15774–15779.

Tang, J., and Q. Zhuang. 2008. Equifinality in parameterization of process-based biogeochemistry models: A significant uncertainty source to the estimation of regional carbon dynamics. Journal of Geophysical Research: Biogeosciences 113:n/a–n/a.

Tang, J., and Q. Zhuang. 2009. A global sensitivity analysis and Bayesian inference framework for improving the parameter estimation and prediction of a process-based Terrestrial Ecosystem Model. Journal of Geophysical Research Atmospheres 114:n/a–n/a.

Tans, P. P., J. A. Berry, and R. F. Keeling. 1993. Oceanic 13C/12C observations: A new window on ocean CO_2 uptake. Global Biogeochemical Cycles 7:353–368.

Tausz-Posch, S., R. M. Norton, S. Seneweera, G. J. Fitzgerald, and M. Tausz. 2013. Will intra-specific differences in transpiration efficiency in wheat be maintained in a high CO2world? A FACE study. Physiologia Plantarum 148:232–245.

Tenhunen, J. D., A. Serra, H. P. C. Sala, R. L. Dougherty, and J. F. Reynolds. 1990. Factors influencing carbon fixation and water use by mediterranean sclerophyll shrubs during summer drought. Oecologia 82:381–393.

Valentini, R., P. de Angelis, G. Matteucci, R. Monaco, S. Dore, and G. E. S. Mucnozza. 1996. Seasonal net carbon dioxide exchange of a beech forest with the atmosphere. Global Change Biology 2:199–207.

Verheijen, L. M., R. Aerts, V. Brovkin, J. Cavender-Bares, J. H. C. Cornelissen, J. Kattge, and P. M. van Bodegom. 2015. Inclusion of ecologically based trait variation in plant functional types reduces the projected land carbon sink in an earth system model. Global Change Biology 21:3074–3086.

Voelker, S. L., F. C. Meinzer, B. Lachenbruch, J. R. Brooks, and R. P. Guyette. 2014. Drivers of radial growth and carbon isotope discrimination of bur oak (*Quercus macrocarpa* Michx.) across continental gradients in precipitation, vapour pressure deficit and irradiance. Plant, Cell & Environment 37:766–779.

Wang, Y.-P., C. M. Trudinger, and I. G. Enting. 2009. A review of applications of model–data fusion to studies of terrestrial carbon fluxes at different scales. Agricultural & Forest Meteorology 149:1829–1842.

Warren, C. R. 2004. The photosynthetic limitation posed by internal conductance to CO_2 movement is increased by nutrient supply. Journal of Experimental Botany 55:2313–2321.

Warren, C. R. 2008. Stand aside stomata, another actor deserves centre stage: the forgotten role of the internal conductance to CO_2 transfer. Journal of Experimental Botany 59:1475–1487.

Weber, J. A., and D. M. Gates. 1990. Gas exchange in *Quercus rubra* (northern red oak) during a drought: analysis of relations among photosynthesis, transpiration, and leaf conductance. Tree Physiology 7:215–225.

White, M. A., P. E. Thornton, S. W. Running, and R. R. Nemani. 2000. Parameterization and sensitivity analysis of the BIOME–BGC terrestrial ecosystem model: net primary production controls. Earth Interactions 4:1–85.

White, J. W. C., B. H. Vaughn, and S. E. Michel 2015. University of Colorado, Institute of Arctic and

Alpine Research (INSTAAR), Stable Isotopic Composition of Atmospheric Carbon Dioxide (13C and 18O) from the NOAA ESRL Carbon Cycle Cooperative Global Air Sampling Network, 1990-2014, Version: 2015-10-26.

Williams, M., et al. 2009. Improving land surface models with FLUXNET data. Biogeosciences 6:1341–1359.

Williams, A. P., J. Michaelsen, S. W. Leavitt, and C. J. Still. 2010. Using tree rings to predict the response of tree growth to climate change in the continental United States during the twenty-first century. Earth Interactions 14:1–20.

Wright, I. J., P. B. Reich, and M. Westoby. 2003. Least-cost input mixtures of water and nitrogen for photosynthesis. American Naturalist 161:98–111.

Wright, I. J., P. B. Reich, J. H. C. Cornelissen, D. S. Falster, P. K. Groom, H. Kouki, L. William, C. H. Lusk, N. Ülo, O. Jacek, O. Noriyuki, P. Hendrik, D. I. Warton, and W. Mark. 2005. Modulation of leaf economic traits and trait relationships by climate. Global Ecology and Biogeography, 14:411–421.

Xu, L., and D. D. Baldocchi. 2003. Seasonal trends in photosynthetic parameters and stomatal conductance of blue oak (*Quercus douglasii*) under prolonged summer drought and high temperature. Tree Physiology 23:865–877.

Zhuang, Q., et al. 2003. Carbon cycling in extratropical terrestrial ecosystems of the Northern Hemisphere during the 20th century: a modeling analysis of the influences of soil thermal dynamics. Tellus Series B 55:751–776.

Data Availability

Data fare available from Figshare: https://doi.org/10.6084/m9.figshare.14328959.v1.

Supporting Information

Additional Supporting Information may be found online at: http://onlinelibrary.wiley.com/doi/10.1002/ecs2.3741/full